# From Binary to Ternary Solvent: Morphology Fine-tuning of D/A Blends in PDPP3T-based Polymer Solar Cells

*Long Ye, Shaoqing Zhang, Wei Ma,* Benhu Fan, Xia Guo, Ye Huang, Harald Ade, and Jianhui Hou**

In the past decade, great successes have been achieved in bulk hetero-junction (BHJ) polymer solar cells (PSCs) in which donor/acceptor (D/A) bi-continuous interpenetrating networks can be formed resulting in a high power conversion efficiency (PCE); in some recent studies, *PCEs* that approach 8% have even been reported.[1,2] In addition to the intrinsic properties of active layer materials, such as bandgaps and molecular energy levels, morphological properties of the D/A blends including crystallinity of polymers, domain size, materials miscibility, hierarchical structures, and molecular orientation are also of great importance for the photovoltaic performance of the devices.[3–8] Therefore, several strategies including slow growth,[9] solvent annealing,[10] thermal annealing,[11] selection of solvent[12] or mixed solvent[13] have been applied to modify or control the morphology of the D/A blends. Among these, binary solvent mixtures have been successfully used in morphology control. For example, the dichlorobenzene (DCB) or chlorobenzene (CB)/1, 8-diiodooctane (DIO) binary solvent system has been widely applied in PSC device fabrication processes. By mixing a few volume percent of DIO with the host solvent (DCB or CB), the efficiencies of many polymers can be improved dramatically.[1,14] Besides DIO, other solvents, like 1,8-octanedithiol (OT),[15] N-methyl-2-pyrrolidone (NMP),[13,16] 1-chloronaphthalene (CN),[16,17] and chloroform (CF),[18,19] can also be used. According to these works, it can be concluded that crystallinity, as well as domain size in the blends can be tuned effectively by using binary solvent mixtures, and thus binary solvent mixtures play a very important role in high performance PSCs.

L. Ye, S. Zhang, B. Fan, X. Guo, Y. Huang, Prof. J. Hou
State Key Laboratory of Polymer Physics and Chemistry
Beijing National Laboratory for Molecular Sciences
Institute of Chemistry
Chinese Academy of Sciences
Beijing 100190, P. R. China
E-mail: hjhzlz@iccas.ac.cn
Dr. W. Ma, Prof. H. Ade
Department of Physics
North Carolina State University
Raleigh, NC 27695, USA
E-mail: wma5@ncsu.edu
L. Ye, X. Guo
Graduate University of Chinese Academy of Sciences
Beijing 100049, P. R. China

DOI: 10.1002/adma.201202855

Conjugated polymers with diketopyrrolopyrrole (DPP) units are widely used in organic photovoltaics to obtain high efficient ultra-low band-gap materials with highly efficient photovoltaic properties.[19–26] As known, photovoltaic performance of the PSCs based on DPP-containing polymers is quite sensitive to morphology of the D/A blends. Therefore, how to select a suitable solvent system to make the solution of the active layer materials is one of the key issues in making highly efficient PSCs based on DPP-containing Polymer/fullerene blends. For instance, when pure CF was used in processing the blend of PDPP3T/$PC_{71}BM$,[21] only a modest *PCE* was obtained, by using a CF/DIO binary solvent, i.e., add small amount of DIO as processing additive during the solution processing of the blend, the *PCE* of the PSC device can be dramatically increased to ~5%. However, considering that PDPP3T has a very broad absorption band covering the range from 400 to 900 nm but the optimum short circuit current density ($J_{SC}$) reported in previous work is 11.8 mA/cm$^2$ only, there should be much space for improving $J_{SC}$ and thus *PCE* of the device.

Compared to binary solvent mixtures, ternary solvent mixtures attracted much less attention from the field of PSCs, though they have been successfully used in other applications, such as liquid chromatography[27] and, electrochemistry,[28] etc. Therefore, it is interesting and also meaningful to investigate the utility of ternary solvent mixtures to PSC active layer fabrication. Herein, a DCB/CF/DIO ternary solvent system was employed to optimize the morphology and thus to improve the photovoltaic performance of the PDPP3T/$PC_{71}BM$ blend films. Since it is quite laborious to do a full scan for three variables in one study, a two-step strategy was adopted for the present solvent investigation as the followings: 1) to optimize photovoltaic performance of PDPP3T-based PSCs by tuning the volume ratio of the two ingredients (DCB and CF) of the binary solvent; 2) to make further improvement of photovoltaic performance by adding another ingredient (DIO) into the binary solvent with the optimal DCB/CF ratio obtained from step 1. The photovoltaic results indicate that photovoltaic performance of the PDPP3T-based PSCs can be improved effectively by this two-step optimization. Furthermore, the morphological evolution of the blends during this two-step optimization process was demonstrated by atomic force microscopy (AFM), resonant soft X-ray scattering (RSoXS) and grazing-incidence wide angle X-ray scattering (GIWAXS) measurements. To the best of our knowledge, this work demonstrates the first successful example for the application of ternary solvent mixture in PSC device fabrication.

As illustrated in **Figure 1**b, a conventional PSC device structure, ITO/PEDOT: PSS (~35 nm)/PDPP3T: $PC_{71}BM$/Ca

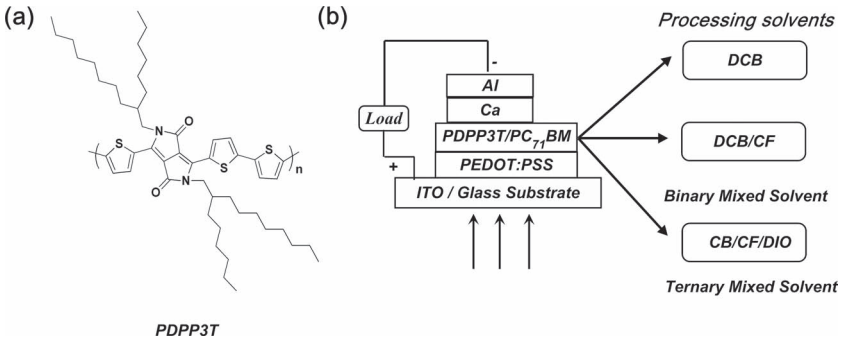


**Figure 1.** (a) Molecular structures of PDPP3T and (b) device structure diagram.

(~20 nm)/Al (~80 nm), was used in this work. The D/A ratio (PDPP3T/$PC_{71}BM$, wt/wt) was optimized by using DCB as the processing solvent prior to the study of mixed solvents, and we found that the optimal D/A ratio is 1:2, which is consistent with the reported work.[21] Then, binary solvent mixtures of DCB and CF were chosen as the processing solvents, and different volume ratios (DCB/CF, v/v), from 1:4 to 4:1, were scanned. *J–V* curves of the PSC devices fabricated by using the binary solvents are shown in Figure S1a, and the photovoltaic results of the PSC devices are listed in Table S1. Furthermore, the data for DCB/DIO (95:5, v/v) are also listed in Table S1 for reference. It can be seen that the best photovoltaic performance with a PCE of 5.38% was recorded with a open circuit voltage ($V_{OC}$) of 0.68 V, a $J_{SC}$ of 11.27 mA/cm$^2$ and a fill factor (*FF*) of 70.08%, when DCB/CF 4:1 (v/v) was used in the binary solvents. The desirable result exceeds the highest *PCE* (4.7%) achieved by CF/DIO co-solvent.[21]

Successively, DIO was used as the third ingredient in the processing solvent mixtures. In order to get a optimum formula of the ternary solvent for achieving high *PCE*, the content of DIO was scanned. DCB and CF mixture with a 4:1 DCB/CF ratio (v/v) was used as the host solvent to make a solution of PDPP3T/$PC_{71}BM$, and then 1%, 3%, 5% or 8% DIO was added prior to spin-coating process. The *J-V* curves of the devices fabricated by using different DIO ratios are plotted in Figure S1b, and the detailed photovoltaic results and device parameters are listed in Table S2. The *J-V* curves of the three representative devices are shown in **Figure 2**a and **Table 1**, and it can be seen that when the ternary solvent (DCB/CF/DIO) was used, $J_{SC}$ of the device can be improved effectively with slightly sacrificing the *FF*. Therefore, the champion device was obtained when a 5% DIO was added during the spin-coating process, and the optimal composition of the ternary solvent is DCB/CF/DIO = 76:19:5 (v/v/v). A *PCE* of 6.71% was recorded from the champion device, which is the highest one for DPP-based BHJ PSCs.

The corresponding external quantum efficiency (*EQE*) curves of the three devices metioned above are shown in Figure 2b. The *EQE* curves indicate that the PSC devices have broad response in the wavelength range from 300 nm to 900 nm. Since the polymer PDPP3T shows weak absorption in short wavelength region, the response of the devices in the region from 400 nm to 600 nm should be due to the absorption of PCBM and the response in long wavelength is ascribed to the polymer. The comparison among these three *EQE* curves reveal that: a) in the device processed by pure DCB, $PC_{71}BM$ works better than the polymer; b) in the device processed by the DCB/CF binary-solvent, the quantum yield from the polymer becomes better while that from $PC_{71}BM$ decreases obviously; c) in the device processed by the ternary solvent, the quantum yield in the whole response region is improved effectively. Additionally, for the device processed from the ternary solvent, the integral current density deduced by *EQE* curve and the global reference spectrum yielded a particularly high $J_{SC}$ of 15.22 mA/cm$^2$. The difference between measured $J_{SC}$ and the calculated current density value is within 5%, indicating that the photovoltaic measurement is reliable.

Grazing-Incidence Wide Angle X-ray scattering (GIWAXS) is used to provide the structural information such as crystallite size, intermolecular distance and crystallite orientation in blend

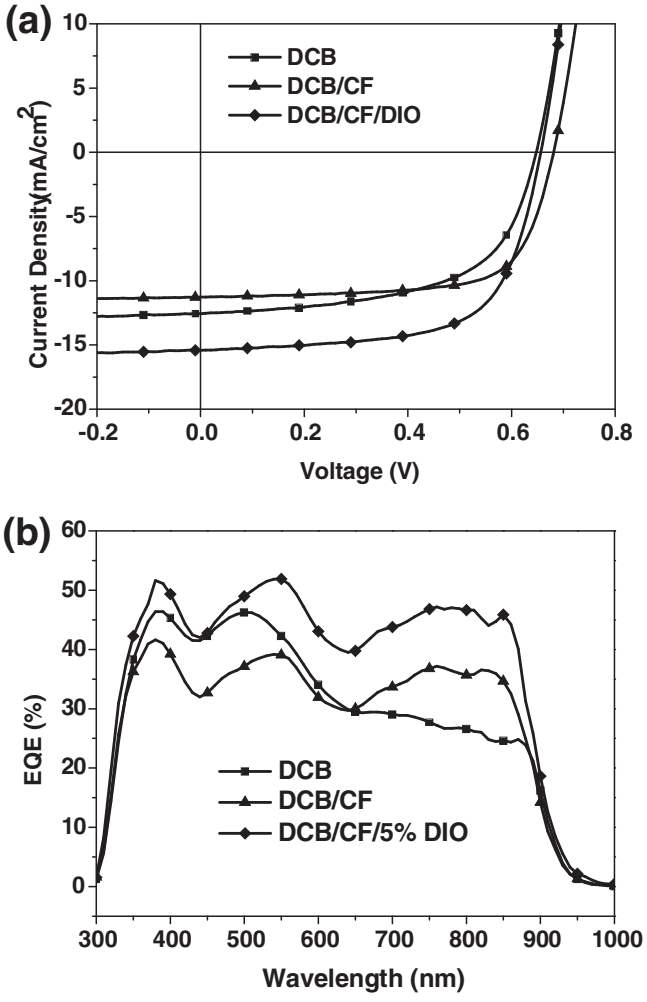


**Figure 2.** *J–V* (a) and *EQE* (b) curves of the PSCs processed from DCB, DCB/CF (4:1, v/v) and DCB/CF/DIO (76:19:5, v/v/v).

**Table 1.** Photovoltaic results of PSCs processed by different solvents.

| Processing Solvent | $V_{OC}$ [V] | $J_{SC}$ [mA/cm$^2$] | *FF* [%] | *PCE* [%] | $R_s$ [Ω cm$^2$] | $\mu_h$[a)] [cm$^2$/(Vs)] |
|---|---|---|---|---|---|---|
| Pure DCB | 0.65 | 12.57 | 59.98 | 4.87 | 10.08 | $5.2 \times 10^{-4}$ |
| DCB/CF (4:1, v/v) | 0.68 | 11.27 | 70.08 | 5.38 | 5.21 | $1.4 \times 10^{-3}$ |
| DCB/CF/DIO (76:19:5, v/v/v) | 0.66 | 15.41 | 65.92 | 6.71 | 5.93 | $3.9 \times 10^{-3}$ |

[a)]Calculated by SCLC method.

films of BHJ PSCs. **Figure 3** shows the out-of-plane (Figure 3b) and in-plane (Figure 3c) GIWAXS profiles of the PDPP3T/$PC_{71}BM$ blend films processed with different solvents. From Figure 3b, it is clear that the (h00) crystallinity of the film processed with DCB was low and only a (100) peak can be observed. When DCB/CF was used, pronounced (100) and (200) reflection peaks are observed. When DCB/CF/DIO was employed, three pronounced reflection peaks, (100), (200), and (300) can be observed clearly, indicating that lamellar stacking of the blend films is further improved. A similar trend can also be observed from the in-plane GIWAXS profiles as shown in Figure 3c. However, it is not thought that charge generation and transport occurs in this direction of polymer crystal and resulting with improving device performance, although an enhanced polymer lamellar stacking is indeed observed. The (010) $\pi$–$\pi$ stacking packing reflection peaks, the direction corresponding to charge transport, are revealed in both Figure 3b and 3c at $q$ near 1.7 Å$^{-1}$, which appeared for all the blend films. We noted that the (010) $\pi$–$\pi$ stacking peaks are more pronounced in out-of plane direction than in-plane direction, which indicates that overall a preferential face-on crystal orientation was formed in blend films. The face-on orientation is considered to be desirable for improved hole transport. However, only minor differences between the three samples are observed. Furthermore, by performing a Scherrer analysis on out-of plane (100) and (010) peaks, the size of crystal and the size of $\pi$–$\pi$ stacks were obtained (see **Table S3**). No significant differences of crystal size are detected among blend films processed with DCB, DCB/CF and DCB/CF/DIO (7.5 nm, 7.8 nm and 8.5 nm, respectively). For the size of $\pi$–$\pi$ stacks, smaller size is found for DCB processed films (ca. 2.0 nm), but little variation is observed for DCB/CF and DCB/CF/DIO (ca. 4.3 nm and 4.5 nm, respectively). This observation mirrors the above discussion that cystallinity can not always be readily correlated to the device performance.

To investigate the nanoscale topography networks, AFM is employed to measure the surface morphology. The height and phase images of the PDPP3T/PCBM blends prepared by using solvents with different compositions are shown in **Figure 4**, and the morphology evolution of the blend films can be well demonstrated. From the comparison of topographies (Figure 4a, 4b and 4c), the mean square surface roughness ($R_q$) of three blend films are 0.86 nm, 2.63 nm, 4.09 nm for the blend films processed from pure DCB, DCB/CF, DCB/CF/5%DIO, respectively. More detailed comparison among the phase images of the films reveals another feature: although nanoscale phase separation can be observed in the film processed by pure DCB, the edges of the domains are very blurry (see Figure 4d), while for the films processed by the

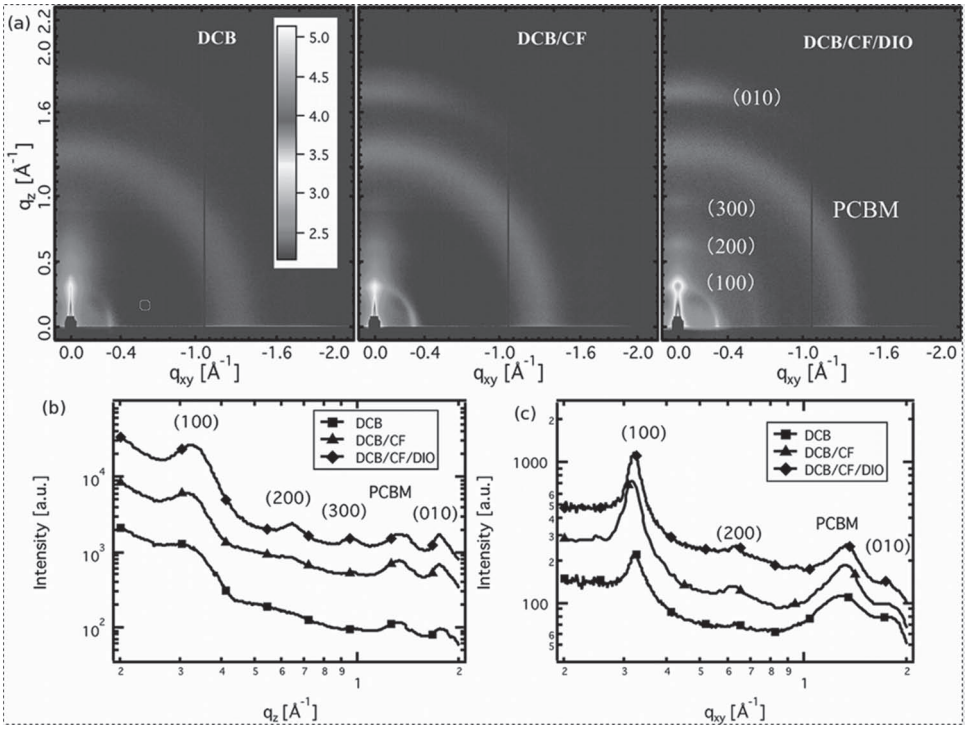


**Figure 3.** 2D pattern (a), out-of-plane (b) and in-plane (c) GIWAXS data of PDPP3T:$PC_{71}BM$ blend films prepared by DCB, DCB/CF (4:1, v/v) and DCB/CF/DIO (76:19:5, v/v/v).

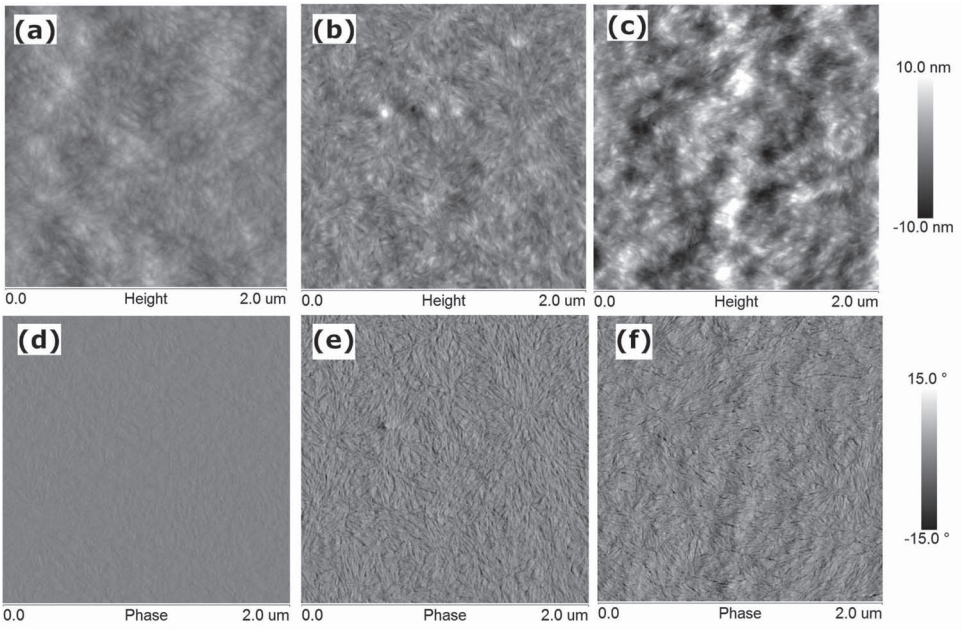


**Figure 4.** AFM topography and phase images (2μm×2μm) of PDPP3T/$PC_{71}BM$ blend films processed by DCB (a, d), DCB/CF (4:1, v/v) (b, e), and DCB/CF/DIO (76:19:5, v/v/v) (c, f).

binary and ternary solvents, sharp and blurry edges of the fibril domains can be observed respectively (see Figure 4e and 4f). Considering that the surface texture needs to be considered with care and might not reflect the bulk morphology, we will show below though that the AFM observation correlate to the sharpness of the domain boundaries inferred from the Porod scaling exponents observed for scattering from the bulk morphology.

Characterization of the bulk morphology, the relative domain purity, and interfacial structure can be achieved with resonant soft X-ray scattering (R-SoXS).[29] A photon energy 284.5 eV was utilized to provide high material contrast between PDPP3T and $PC_{71}BM$ (see Figure S3). **Figure 5** shows the R-SoXS data for PDPP3T:$PC_{71}BM$ blends processed with DCB, DCB/CF and DCB/CF/DIO solvents, along with a fit of the high *q*-data to a power law and a background to account for x-ray fluorescence (For details, see Supporting Information). We note that the location of the peak, the scattering intensities and the distribution of R-SoXS patterns are clearly sensitive to which processing solvent is used. The location of peaks represents the dominant domain spacing of donor to donor or from acceptor to acceptor phases. The scattering profiles represent the domain size distribution at low and medium q, i. e. structure factor, whereas at very high *q*, the scaling of the intensity relates to the sharpness of the interfaces (Porod regime). It was observed that overall, the bulk morphology exhibits larger domains than observed with AFM. Specifically, the PDPP3T/$PC_{71}BM$ blend films processed by DCB had the coarsest morphology with a dominant domain spacing of 81 nm. In contrast, when the binary (DCB/CF) and the ternary (DCB/CF/DIO) solvent were used in the film fabrication, the dominant domain spacing was reduced to ~71 nm. Notably, the DCB sample has the highest scattering intensity at low *q* and a dispersion of domains size, whereas the DCB/CF/DIO samples has the highest intensity at high *q*, and the DCB/CF samples the most narrow dispersion of size.

The relative domain purity of an assumed two-phase system can be extracted by integrating scattering profiles via total scattering intensity (*TSI*)[30] (see Supporting Information for details). The purer the domains are, the higher the *TSI*. Relative *TSI* values of 0.79, 0.93, and 1 are obtained for DCB, binary and ternary solvents, respectively. The domains become more pure when DCB is mixed with CF and further improvement of relative domain purity can be achieved by adding DIO.

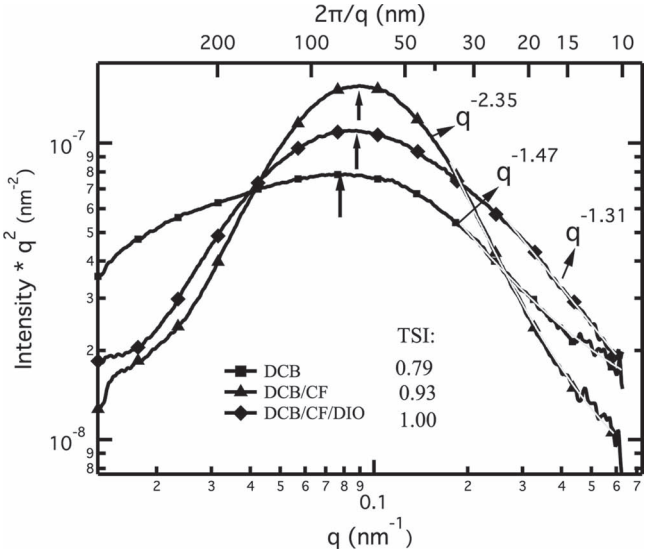


**Figure 5.** R-SoXS information of PDPP3T/$PC_{71}BM$ blend films prepared at various conditions: DCB, DCB/CF (4:1, v/v), DCB/CF/DIO (76:19:5, v/v/v). The peak locations are marked by the arrows. The total scattering intensity and the scaling exponents at high *q* are also indicated.

The scaling at high $q$ is also rather informative. Two situations are observed. The DCB/CF sample exhibit scaling exponent of –4.35, which indicates that the interfaces are smooth and rather sharp, i.e. only slightly interdiffused (an ideal sharp interface has a scaling exponent of –4).[31,32] The pure DCB sample and the DCB/CF/DIO samples show exponents of approximately –3.31, while indicates that the interfaces in these samples are somewhat rough and possibly fractal in nature, leading to access scattering relative to perfectly sharp and smooth interface. The interface characteristics appear to be driven by CF when CF is added to DCB (see Figure S4), the effect of which is negated and the interface structure reverts back to that of DCB when the DIO is added.

Overall, three parameters have been extracted from the R-SoXS data: The dominant domain size and domain size distribution, the overall relative domain purity, and the nature of the donor-acceptor interface. We will discuss these in relation to the $J_{SC}$ and *FF* in the context of exciton dissociation efficiency, charge recombination and charge transport. It is generally assumed that smaller domains are more favorable for high exciton dissociation efficiency, as the exciton diffusion length is typically only about 10 nm.[33–35] Also, rough interfaces with an increase in interfacial area provide improved exciton dissociation efficiency. However, depending on the length scale of this roughness, it might also enhance bi-molecular recombination if the charges are not transported efficiently to the electrodes. This competing effect was previously investigated in bilayer model systems of PFB/F8BT by Yan et al.[8] In that particular case, it was found and supported by Monte Carlo simulations, that sharp interfaces are best, and the recombination outweighs the increase in area. Lastly, domain purity is important as impure domains should lead to enhanced bi-molecular recombination and reduced charge transport.

Then the following overall picture emerges, as illustrated in **Figure 6**. DCB leads to domains that are the largest, with a wide distribution of domains size, with the most impure domains and somewhat rough interfaces. This leads to a high exciton dissociation efficiency, hence good $J_{SC}$, but at a cost of bi-molecular recombination and reduction in FF. Generally, the PCBM domains are rather pure and impurity of the domains is generally due to PCBM dispersed in the amorphous portion of the polymer.[30] This would be consistent with the relative bad *EQE* of the polymer as shown in Figure 2b. The addition of CF to DCB leads to a marked improvement in domain purity and reduced domain size with sharper interfaces. Therefore, the hole mobility ($\mu_h$) of the blend was improved from $5.2 \times 10^{-4}$ to $1.4 \times 10^{-3}$ $cm^2/(V \cdot s)$, and this leads to the best *FF*. However, the overall domain size is too large for efficient charge separation, and the $J_{SC}$ is not much changed relative to DCB alone. With DIO added to DCB/CF, the overall domain size is not changing much, but the rougher interfaces provide a shorter average distance from the average location of the photon absorption site to the donor/acceptor interface. This enhances exciton dissociation and thus $J_{SC}$. The slightly increased purity is however negated by the enhanced bi-molecular recombination at the rough interfaces with a concomitant reduction in *FF*. Consequently, the series resistance ($R_s$) decreases from the initial value of 10.08 to 5.21 $\Omega \cdot cm^2$ and then slightly increases to 5.93 $\Omega \cdot cm^2$,when the processing solvent successively change from single solvent to ternary solvent. This would be analogous to the situation observed for PFB/F8BT.[8] Monte Carlo simulations and a more detailed study of the scattering scaling behavior for a larger range of solvents would be helpful to further elucidate the relative importance of the interface. Presently, even just the raw data clearly indicates that the interfaces are roughly of two types and detailed characterization is outside the scope of this first report of the use of ternary solvent mixture.

In conclusion, by incorporating three functional solvents as processing solvent for the first time, we are able to create

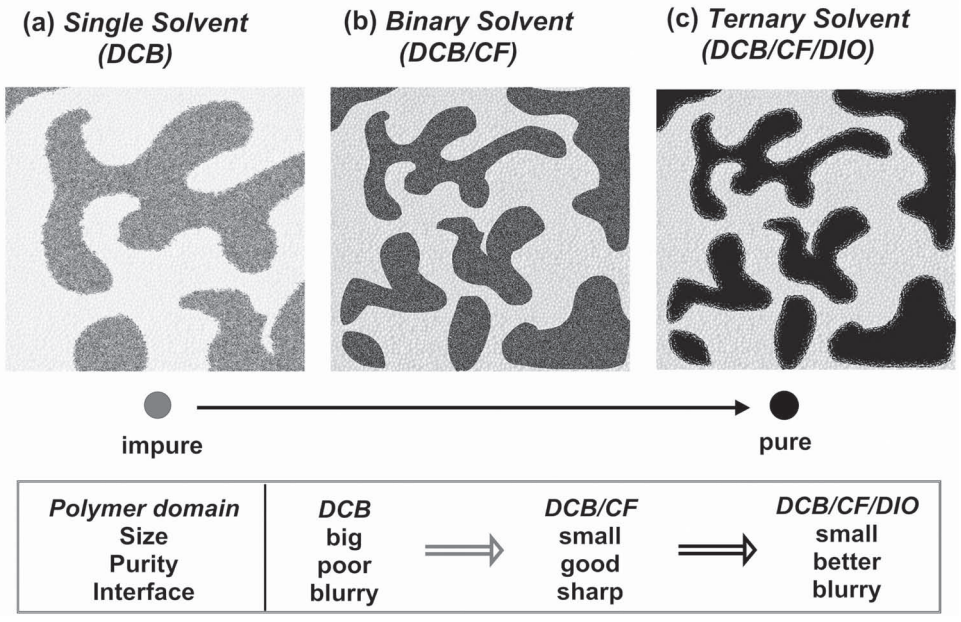


**Figure 6.** Morphology evolution of the PDPP3T/$PC_{71}BM$ blends prepared by different solvents.

efficient BHJ PSC devices with PDPP3T: $PC_{71}BM$ as active layer. The PCE of the device prepared by optimal condition reached 6.71%, which is a remarkable result for the PSC based on DPP-based polymers. Furthermore, the morphology of the PDPP3T/$PC_{71}BM$ blend film was successfully optimized by the application of a DCB/CF/DIO (76:19:5, v/v/v) ternary solvent system for solution processing and therefore the PCE of PDPP3T/PCBM-based PSC devices can be improved effectively. By using AFM, R-SoXS and GIWAXS measurements, the evolution of the morphology from the pure solvent (DCB) to the binary mixed solvent (DCB/CF) and then to ternary mixed solvent (DCB/CF/DIO) is well demonstrated. The advantage of ternary mixed solvents treatment is the combination of two steps tuning of morphology, and hence long-range ordered structure with favorable domain size and good domain purity as well as the rougher domain interfaces in the PDPP3T:$PC_{71}BM$ blend can be realized.

More importantly, this method could pave a path to the optimization of other high performance photovoltaic materials. Further advances in efficiency can be expected for the PDPP3T/PCBM system when the domain size can be further reduced upon the exciton diffusion length of 10–20 nm. The best strategy appears to be use of a third co-solvent that preserves the *FF*, sharpness of interface, and purity of the DCB/CF solvent mixture, but leads to smaller domains to achieve higher $J_{SC}$. Even though DIO produced the best results, other solvent additives need to be explored.

## Experimental Section

*Materials*: PDPP3T ($M_n$ = 780K, PDI = 3.25, GPC method by using chloroform as eluent at 45 °C) was purchased from Solarmer Material Inc and $PC_{71}BM$ was purchased from Nano-C Inc. The ultradry solvents used in device fabrication process were purchased from Alfa Aesar. The other chemicals are commercially available products and were used without any further purification.

*Measurements*: GIWAXS, R-SoXS, and reference spectroscopy measurements were performed at beamline 7.3.3.,[36] beamline 11.0.1.2.,[37] and beamline 5.3.2.2, respectively at the Advanced Light Source, Lawrence Berkeley National Laboratory, Berkeley, CA. Morphology was performed on a Nanoscope V (Vecco) Atom Force Microscopy in the tapping mode. IPCE measurements were performed at Solar Cell Spectral Response Measurement System QE-R3011 (Enli Technoloy Co., Ltd.). The *J-V* curves were measured under an illumination of 100 mW·cm$^{-2}$ AM 1.5G using a XES-70S1 (SAN-EI Electric Co., Ltd.) solar simulator (AAA grade, 70 mm × 70 mm photo-beam size). 2 × 2 cm Monocrystalline silicon reference cell (SRC-1000-TC-QZ) was purchased from VLSI Standards Inc.

## Supporting Information

Supporting Information is available from the Wiley Online Library or from the author.

## Acknowledgements

The authors would like to acknowledge the financial support from National high technology research and development program 863 (2011AA050523), Chinese Academy of Sciences, Ministry of Science and Technology of China, NSFC (Nos. KGCX2-YW-399+9-1, S2012GR0224, 51173189). R-SoXS and GIWAXS measurements and analysis by Dr. Wei Ma and Prof. Harald Ade are supported by the US Department of Energy, Office of Science, Basic Energy Science, Division of Materials Science and Engineering under contract DE-FG02-98ER45737. X-ray data is acquired at the Advanced Light Source, which is supported by the the Director, Office of Science, Office of Basic Energy Sciences, of the U.S. Department of Energy under Contract No. DE-AC02-05CH11231.

Received: July 14, 2012
Revised: August 12, 2012
Published online: September 19, 2012

[1] a) Y. Huang, X. Guo, F. Liu, L. J. Huo, Y. N. Chen, T. P. Russell, C. C. Han, Y. F. Li, J. H. Hou, *Adv. Mater.* **2012**, 24,3383; b) C. M. Amb, S. Chen, K. R. Graham, J. Subbiah, C. E. Small, F. So, J. R. Reynolds, *J. Am. Chem. Soc.* **2011**, *133*, 10062; c) S. C. Price, A. C. Stuart, L. Q. Yang, H. X. Zhou, W. You, *J. Am. Chem. Soc.* **2011**, *133*, 4625; d) T. Y. Chu, J. P. Lu, S. Beaupre, Y. G. Zhang, J. R. Pouliot, S. Wakim, J. Y. Zhou, M. Leclerc, Z. Li, J. F. Ding, Y. Tao, *J. Am. Chem. Soc.* **2011**, *133*, 4250; e) L. J. Huo, S. Q. Zhang, X. Guo, F. Xu, Y. F. Li, J. H. Hou, *Angew. Chem. Int. Ed.* **2011**, *50*, 9697.

[2] a) Z. C. He, C. M. Zhong, X. Huang, W. Y. Wong, H. B. Wu, L. W. Chen, S. J. Su, Y. Cao, *Adv. Mater.* **2011**, *23*, 4636; b) L. T. Dou, J. B. You, J. Yang, C. C. Chen, Y. J. He, S. Murase, T. Moriarty, K. Emery, G. Li, Y. Yang, *Nat. Photo.* **2012**, *6*, 180; c) X. H. Li, W. C. H. Choy, L. J. Huo, F. X. Xie, W. E. I. Sha, B. F. Ding, X. Guo, Y. F. Li, J. H. Hou, J. B. You, Y. Yang, *Adv. Mater.* **2012**, 24,3046; d) C. E. Small, S. Chen, J. Subbiah, C. M. Amb, S. W. Tsang, T. H. Lai, J. R. Reynold, F. So, *Nat. Photo.* **2012**, *6*, 115.

[3] L. M. Chen, Z. R. Hong, G. Li, Y. Yang, *Adv. Mater.* **2009**, *21*, 1434.

[4] B. A. Collins, J. Tumbleston, H. Ade, *J. Phys. Chem. Lett.* **2011**, *2*, 3135.

[5] B. A. Collins, E. Gann, L. Guignard, X. X. He, C. R. McNeill, H. Ade, *J. Phys. Chem. Lett.* **2010**, *1*, 3160.

[6] B. A. Collins, J. E. Cochran, H. Yan, E. Gann, C. Hub, R. Fink, C. Wang, T. Schuettfort, C. R. McNeill, M. L. Chabinyc, H. Ade, *Nat. Mater.* **2012**, *11*, 536.

[7] W. Chen, T. Xu, F. He, W. Wang, C. Wang, J. Strzalka, Y. Liu, J. G. Wen, D. J. Miller, J. H. Chen, K. L. Hong, L. P. Yu, S. B. Darling, *Nano Lett.* **2011**, *11*, 3707.

[8] H. P. Yan, S. Swaraj, C. Wang, I. Hwang, N. C. Greenham, C. Groves, H. Ade, C. R. McNeill, *Adv. Funct. Mater.* **2010**, *20*, 4329.

[9] G. Li, V. Shrotriya, J. S. Huang, Y. Yao, T. Moriarty, K. Emery, Y. Yang, *Nat. Mater.* **2005**, *4*, 864.

[10] G. Li, Y. Yao, H. Yang, V. Shrotriya, G. Yang, Y. Yang, *Adv. Funct. Mater.* **2007**, *17*, 1636.

[11] a) F. Padinger, R. S. Rittberger, N. S. Sariciftci, *Adv. Funct. Mater.* **2003**, *13*, 85; b) W. L. Ma, C. Y. Yang, X. Gong, K. Lee, A. J. Heeger, *Adv. Funct. Mater.* **2005**, *15*, 1617.

[12] S. E. Shaheen, C. J. Brabec, N. S. Sariciftci, F. Padinger, T. Fromherz, J. C. Hummelen, *Appl. Phys. Lett.* **2001**, *78*, 841.

[13] Y. Yao, J. H. Hou, Z. Xu, G. Li, Y. Yang, *Adv. Funct. Mater.* **2008**, *18*, 1783.

[14] J. K. Lee, W. L. Ma, C. J. Brabec, J. Yuen, J. S. Moon, J. Y. Kim, K. Lee, G. C. Bazan, A. J. Heeger, *J. Am. Chem. Soc.* **2008**, *130*, 3619.

[15] J. Peet, J. Y. Kim, N. E. Coates, W. L. Ma, D. Moses, A. J. Heeger, G. C. Bazan, *Nat. Mater.* **2007**, *6*, 497.

[16] X. Guo, C. H. Cui, M. J. Zhang, L. J. Huo, Y. Huang, J. H. Hou, Y. F. Li, *Energy Environ. Sci.* **2012**, 5,7943.

[17] C. V. Hoven, X. D. Dang, R. C. Coffin, J. Peet, T. Q. Nguyen, G. C. Bazan, *Adv. Mater.* **2010**, *22*, E63.

[18] F. L. Zhang, K. G. Jespersen, C. Bjorstrom, M. Svensson, M. R. Andersson, V. Sundstrom, K. Magnusson, E. Moons, A. Yartsev, O. Inganas, *Adv. Funct. Mater.* **2006**, *16*, 667.

[19] F. Liu, Y. Gu, C. Wang, W. Zhao, D. Chen, A. L. Briseno, T. P. Russell, *Adv. Mater.* **2012**, 24,3947.
[20] M. M. Wienk, M. Turbiez, J. Gilot, R. A. J. Janssen, *Adv. Mater.* **2008**, *20*, 2556.
[21] J. C. Bijleveld, A. P. Zoombelt, S. G. J. Mathijssen, M. M. Wienk, M. Turbiez, D. M. de Leeuw, R. A. J. Janssen, *J. Am. Chem. Soc.* **2009**, *131*, 16616.
[22] J. C. Bijleveld, V. S. Gevaerts, D. Di Nuzzo, M. Turbiez, S. G. J. Mathijssen, D. M. de Leeuw, M. M. Wienk, R. A. J. Janssen, *Adv. Mater.* **2010**, *22*, E242.
[23] C. H. Woo, P. M. Beaujuge, T. W. Holcombe, O. P. Lee, J. M. J. Fréchet, *J. Am. Chem. Soc.* **2010**, *132*, 15547.
[24] H. Bronstein, Z. Y. Chen, R. S. Ashraf, W. M. Zhang, J. P. Du, J. R. Durrant, P. S. Tuladhar, K. Song, S. E. Watkins, Y. Geerts, M. M. Wienk, R. A. J. Janssen, T. Anthopoulos, H. Sirringhaus, M. Heeney, I. McCulloch, *J. Am. Chem. Soc.* **2011**, *133*, 3272.
[25] A. T. Yiu, P. M. Beaujuge, O. P. Lee, C. H. Woo, M. F. Toney, J.M. Fréchet, *J. Am. Chem. Soc.* **2012**, *134*, 2180.
[26] L. T. Dou, J. Gao, E. Richard, J. B. You, C. C. Chen, K. C. Cha, Y. J. He, G. Li, Y. Yang, *J. Am. Chem. Soc.* **2012**, *134*, 10071.
[27] a) G. Jones, *J. Chromatogr.* **1980**, *221*, 27; b) J. A. Martinez-Pontevedra, L. Pensado, M. C. Casais, R. Cela, *Anal. Chim. Acta.* **2004**, *515*, 127.
[28] D. Peramunage, D. M. Pasquariello, K. M. Abraham, *J. Electrochem. Soc.* **1995**, *142*, 1789.
[29] a) S. Swaraj, C. Wang, H. Yan, B. Watts, J. Luning, C. R. McNeill, H. Ade, *Nano Lett.* **2010**, *10*, 2863; b) H. Yan, B. A. Collins, E. Gann, C. Wang, H. Ade, C. R. McNeill, *ACS Nano* **2012**, *6*, 677.
[30] B. A. Collins, Z. Li, J. Tumbleston, E. Gann, C. R. McNeill, H. Ade, *Adv. Energy. Mater.* **2012**, DOI:10.1002/aenm.201200377.
[31] H. Brumberger, *Modern Aspects of Small-Angle Scattering*. Kluwer Academic Publishers, Dordrecht, **1995**, 45, 463.
[32] G. Porod, *Colloid Polym. Sci.* **1952**, *125*, 108–122.
[33] C. Deibel, V. Dyakonov, *IEEE J. Selected Topics Quantum Electron.* **2010**, *16*, 1517–1527.
[34] R. R. Lunt, N. C. Giebink, A. A. Belak, J. B. Benziger, S. R. Forrest, *J. Appl. Phys.* **2009**, *105*, 053711.
[35] P. E. Shaw, A. Ruseckas, I. D. W. Samuel, *Adv. Mater.* **2008**, *20*, 3516.
[36] A. Hexemer, W. Bras, J. Glossinger, E. Schaible, E. Gann, R. Kirian, A. MacDowell, M. Church, B. Rude, H. Padmore, *J. Phys. Conf. Ser.* **2010**, *247*, 012007.
[37] E. Gann, A. Young, B. A. Collins, H. Yan, J. Nasiatka, H. A. Padmore, H. Ade, A. Hexemer, C. Wang, *Rev. Sci. Instrum.* **2012**, *83*, 045110.